IEEE Access
Multidisciplinary | Rapid Review | Open Access Journal

Received September 12, 2018, accepted September 28, 2018, date of publication October 4, 2018, date of current version October 29, 2018.

Digital Object Identifier 10.1109/ACCESS.2018.2873688

Computer-Aided Tuning of Highly Lossy Microwave Filters Using Complex Coupling Matrix Decomposition and Extraction

RANJAN DAS[1,2], (Student Member, IEEE), QINGFENG ZHANG[1], (Senior Member, IEEE), ABHISHEK KANDWAL[1], (Member, IEEE), HAIWEN LIU[3], (Senior Member, IEEE), AND YIFAN CHEN[4], (Senior Member, IEEE)

[1]Department of Electronics and Electrical Engineering, Southern University of Science and Technology, Shenzhen 518055, China
[2]Electrical Engineering Department, IIT Bombay, Mumbai 400076, India
[3]School of Electronic and Information Engineering, Xi'an Jiaotong University, Xi'an 710049, China
[4]Faculty of Science and Engineering, The University of Waikato, Hamilton 3216, New Zealand

Corresponding author: Qingfeng Zhang (zhang.qf@sustc.edu.cn)

This work was supported in part by the National Natural Science Foundation of China under Grant 61871207, in part by the Guangdong Natural Science Funds for Distinguished Young Scholar under Grant 2015A030306032, in part by the Talent Support Project of Guangdong under Grant 2016TQ03X839, and in part by the Shenzhen Science and Technology Innovation Committee Funds under Grant KQJSCX20160226193445, Grant JCYJ20160301113918121, and Grant JSGG20160427105120572.

ABSTRACT Lossy filters have broad applications in satellite communication systems. This paper proposes an efficient tuning method, based on complex coupling matrix decomposition and extraction, for highly lossy filters. Interestingly, it shows that the proposed decomposition technique preserves the scattering parameters of the original coupling matrix. A simple and efficient tuning algorithm is provided and illustrated with a four-pole lossy Chebyshev filter example. The experimental demonstration is finally presented to validate the proposed tuning technique.

INDEX TERMS Coupling matrix, decomposition, extraction, tuning, lossy filter.

I. INTRODUCTION

Microwave filters have broad applications in modern communication systems. Lossless filters are generally synthesized and designed using coupling matrix techniques [1]–[4]. Tuning of microwave filters requires huge efforts. Initially, they were accomplished by human operators, which is not only time consuming but also cost ineffective. Gradually it was replaced by computerized automated tuning (CAT) method [5]–[7], which is very useful for tuning of complicated higher-order filters. CAT-based sequential tuning method [8] is very effective for in-line filters but less effective for filters having complex or multiple cross couplings. To overcome such limitations, researchers developed fuzzy logic based tuning algorithm [9]–[11]. Additionally, human experience or linguistic rule based fuzzy controller was proposed in [12]–[14] for accurate and robust tuning. Ring resonator based dual mode bandpass filter tuning method was described in [15]. Further, bond wires based passive filters tuning method was proposed in [16]. Inspite of great effort made by researchers, all these auto tuning techniques are limited to lossless filters only.

Lossy filters are widely applied in satellite communications where inband flatness and frequency selectivity rather than the absolute loss are the leading parameters one needs to concern. Recently, lossy filters based on complex coupling matrix are also applied to the design of negative group delay devices [17]. Tuning of such filters are very different from lossless filters. In [18], a tuning technique based on admittance parameters was explored for even Q_u resonators. In [19], tuning of lossy filters with uneven Q_u resonators were proposed. All of these techniques are only limited to filters having small losses and concentrating all the losses on the resonators. For highly lossy filters and the cases with complex couplings (e.g. [17]), no efficient tuning techniques are available.

This paper proposes a complete and systematic tuning technique for highly lossy filters. In the tuning process, it employs coupling matrix decomposition and extraction, which exhibits great benefits in dealing with complex coupling matrices. The decomposition technique results in two matrices that have one-to-one correspondence with the physical implementation. The extraction technique has been

presented in [19], which is however very abstract. This paper presents an extension to [19]. Major contributions in addition to [19] include: 1) we illustrate the tuning principle and procedure in more details and more examples; 2) a complex coupling matrix decomposition technique is added to ease the physical implementation; 3) physical implementation and experimental validation are added to verify the proposed technique; 4) synthesis of lossy filters is recalled to introduce how a complex coupling matrix is resulted, which help readers understand why complex coupling matrix is important.

This paper is organized as follows. Sec. II firstly recalls the synthesis of lossy filters, and subsequently introduces a decomposition technique to deal with the complex coupling matrix, and finally presents the tuning procedure. Sec. III illustrates the tuning technique step by step using an example, followed by an experimental validation. Final conclusion is drawn in Sec. IV.

II. SYNTHESIS AND TUNING OF LOSSY FILTERS

Since filter tuning is always related to its synthesis, we will briefly introduce the synthesis approach for lossy filters before going to the tuning part. In between, we also present a unique coupling matrix decomposition technique, which plays an important role in the tuning of highly lossy filters.

A. SYNTHESIS OF LOSSY FILTERS

The scattering matrix of a filter is given by [3],

$$\begin{bmatrix} S_{11} & S_{12} \\ S_{21} & S_{22} \end{bmatrix} = \frac{1}{E(s)} \begin{bmatrix} F_{11}(s) & P(s) \\ P(s) & F_{22}(s) \end{bmatrix}, \qquad (1)$$

where E, P, F_{11}, and F_{22} are characteristic polynomials. E is a Hurwitz polynomial whose roots are on the left part of complex frequency plane.

TABLE 1. Characteristic polynomials of a lossless four-pole elliptic filter.

$P(s)$	$j0.6377s^2 + j1.4348$
$F_{11}(s) = F_{22}(s)$	$s^4 + 1.2025s^2 + 0.2025$
$E(s)$	$s^4 + 1.81s^3 + 2.94s^2 + 2.45s + 1.47$

The lossy filter synthesis begins with a lossless filter synthesis [20]. Firstly, characteristic polynomials of lossless filters are synthesized using the classic approach in [4]. For better illustration, let us consider a four pole lossless Elliptic filter with transmission zeros at $\Omega = \pm 1.5$ and maximum return loss of 17.5 dB within $\Omega \in [-1\ 1]$. The synthesized characteristic polynomials are given in Tab. 1 and the corresponding magnitude responses are shown in Fig. 1. Once having the lossless filter in Tab. 1, one subsequently incorporates the loss into the scattering parameters by multiplying an attenuation constant, $K = 0.56$ corresponding to a 5-dB insertion loss, with the obtained $P(s)$, $F_{11}(s)$ and $F_{22}(s)$ in Tab. 1 [20]. The resultant characteristics polynomials are shown in Tab. 2, and its magnitude responses are plotted in Fig. 2.

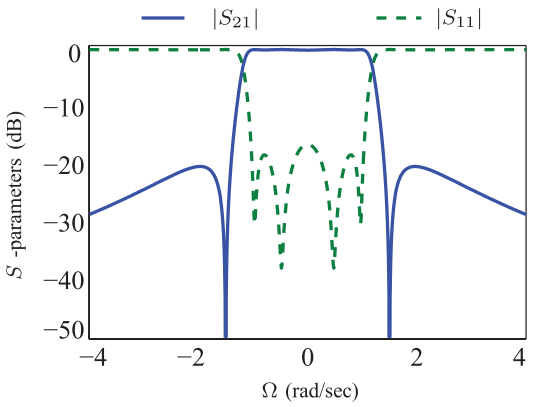

FIGURE 1. Magnitude responses of the lossless four-pole Elliptic filter in Tab. 1.

TABLE 2. Characteristic polynomials of a four-pole lossy elliptic filter.

K	0.56
$\hat{P}'(s)$	$j0.3571s^2 + j0.8035$
$F'_{11}(s) = F'_{22}(s)$	$0.56s^4 + 0.6734s^2 + 0.1134$
$E(s)$	$s^4 + 1.81s^3 + 2.94s^2 + 2.45s + 1.47$

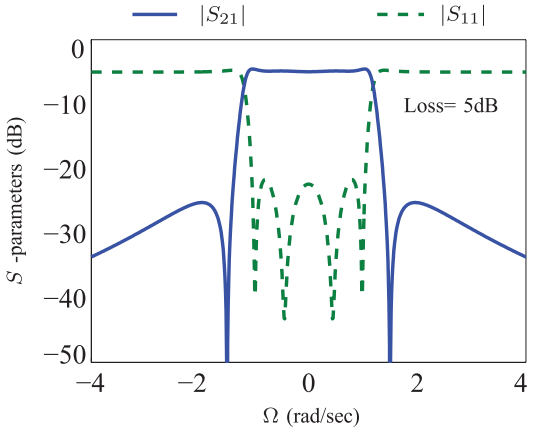

FIGURE 2. Magnitude responses of the lossy four-pole Elliptic filter in Tab. 2.

Once having the characteristic polynomials of the lossy filter in Fig. 2, one subsequently computes the corresponding coupling matrix using the technique in [20]. Fig. 3 shows the resultant coupling matrix along with the coupling topology. Note that the losses are concentrated on resonators 1 and 4 as well as source and load, whereas resonators 2 and 3 are purely lossless. Also, all the coupling values are real. Tuning of such non-uniform Q_u lossy filters has been described in [18] and [19]. But in general lossy filters with uniform Q_u resonators are preferable due to the ease of design and fabrication. Therefore, one needs to equalize the loss among all the resonators using the hyperbolic rotation technique provided in [21]. The loss equalized coupling matrix and coupling topology are shown in Fig. 4. Note that, as a result of loss equalization, lossy (imaginary) cross couplings appear in the coupling matrix.

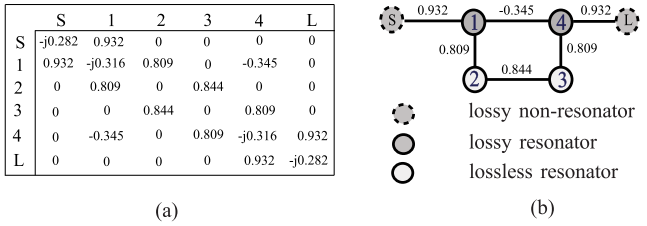

	S	1	2	3	4	L
S	-j0.282	0.932	0	0	0	0
1	0.932	-j0.316	0.809	0	-0.345	0
2	0	0.809	0	0.844	0	0
3	0	0	0.844	0	0.809	0
4	0	-0.345	0	0.809	-j0.316	0.932
L	0	0	0	0	0.932	-j0.282

(a) (b)

FIGURE 3. A 4th order lossy Elliptic filter (Table 2) (a) coupling matrix, and (b) coupling topology before loss equalization.

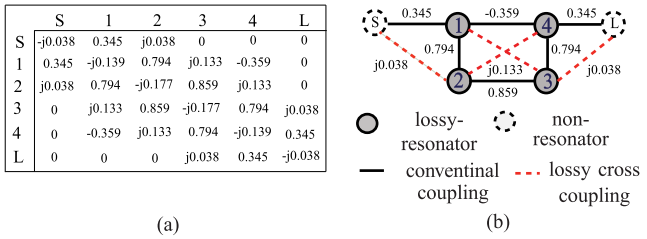

	S	1	2	3	4	L
S	-j0.038	0.345	j0.038	0	0	0
1	0.345	-j0.139	0.794	j0.133	-0.359	0
2	j0.038	0.794	-j0.177	0.859	j0.133	0
3	0	j0.133	0.859	-j0.177	0.794	j0.038
4	0	-0.359	j0.133	0.794	-j0.139	0.345
L	0	0	0	j0.038	0.345	-j0.038

(a) (b)

FIGURE 4. Uniform lossy four-pole Elliptic filter (after loss equalization of Fig. 3.) (a) coupling matrix, and (b) coupling topology after loss equalization having input and output coupling of 0.3676.

TABLE 3. Characteristic polynomials of a four-pole lossy Chebyshev filter.

$P'(s)$	$j0.594$
$F'_{11}(s) = F'_{22}(s)$	$0.475s^4 + 0.475s^2 + 0.059$
$E(s)$	$s^4 + 2.1436s^3 + 3.2974s^2 + 2.8281s + 1.25$

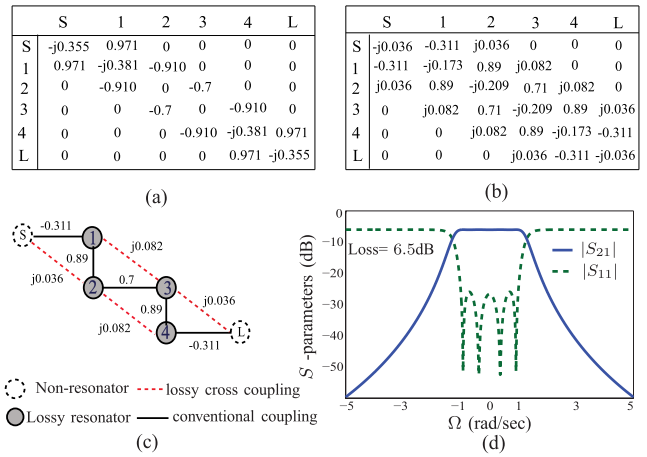

	S	1	2	3	4	L
S	-j0.355	0.971	0	0	0	0
1	0.971	-j0.381	-0.910	0	0	0
2	0	-0.910	0	-0.7	0	0
3	0	0	-0.7	0	-0.910	0
4	0	0	0	-0.910	-j0.381	0.971
L	0	0	0	0	0.971	-j0.355

(a)

	S	1	2	3	4	L
S	-j0.036	-0.311	j0.036	0	0	0
1	-0.311	-j0.173	0.89	j0.082	0	0
2	j0.036	0.89	-j0.209	0.71	j0.082	0
3	0	j0.082	0.71	-j0.209	0.89	j0.036
4	0	0	j0.082	0.89	-j0.173	-0.311
L	0	0	0	j0.036	-0.311	-j0.036

(b)

(c) (d)

FIGURE 5. A four-pole lossy Chebyshev filter (Table 3) (a) coupling matrix with unequal Q_u, (b) loss equalized coupling matrix, (c) corresponding coupling topology, and (d) magnitude responses with input/output couplings of 0.3184.

Without loss of generality, we also include another example, a four-pole Chebyshev filter without any transmission zeros, with a 6.5 dB insertion loss. Following a similar procedure, one obtains the characteristic polynomials in Tab. 3. The coupling matrices and coupling topology are shown in Fig. 5. Again, the loss equalized coupling matrix in Fig. 5(b) contains several complex cross couplings.

Therefore, in the design of lossy filters, one usually arrives at complex coupling matrices as the ones in Figs. 4 and 5.

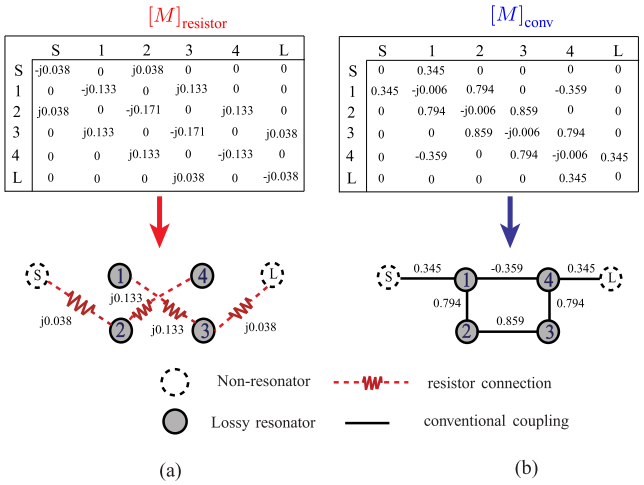

$[M]_{\text{resistor}}$

	S	1	2	3	4	L
S	-j0.038	0	j0.038	0	0	0
1	0	-j0.133	0	j0.133	0	0
2	j0.038	0	-j0.171	0	j0.133	0
3	0	j0.133	0	-j0.171	0	j0.038
4	0	0	j0.133	0	-j0.133	0
L	0	0	0	j0.038	0	-j0.038

$[M]_{\text{conv}}$

	S	1	2	3	4	L
S	0	0.345	0	0	0	0
1	0.345	-j0.006	0.794	0	-0.359	0
2	0	0.794	-j0.006	0.859	0	0
3	0	0	0.859	-j0.006	0.794	0
4	0	-0.359	0	0.794	-j0.006	0.345
L	0	0	0	0	0.345	0

(a) (b)

FIGURE 6. Decomposed coupling matrices of a four-pole lossy Elliptic filter (Fig. 4) (a) resistor connection matrix $[M]_{\text{resistor}}$ with diagram, and (b) residue coupling matrix $[M]_{\text{conv}}$ with corresponding coupling diagram.

In these cases, the conventional tuning techniques in [18] and [19] are not applicable. So, we propose a new tuning technique to handle this type of complex coupling matrices. Before going to any detail of the tuning procedure, we will firstly introduce, in the next section, a decomposition technique that is a vital step for tuning such lossy filters.

B. COUPLING MATRIX DECOMPOSITION

In the design of lossy filters, one needs to deal with complex coupling matrices, such as Figs. 4 and 5. Here, we decompose the complex coupling matrix into two parts, i.e.

$$[M] = [M]_{\text{resistor}} + [M]_{\text{conv}}\,, \tag{2}$$

where $[M]_{\text{resistor}}$ represents the series resistive connection among resonators, and $[M]_{\text{conv}}$ is the residue coupling matrix containing real couplings only. Such a decomposition is finished by taking all the imaginary coupling coefficients out of the off-diagonal entries of a complex coupling matrix to form the resistive matrix and leaving the rest to form the conventional coupling matrix. Note that decomposition (2) is not a trivial operation as it performs in such a way that each sub-matrix within $[M]_{\text{resistor}}$ will turn out to be a series resistor following (3) which will be illustrated later. Such a decomposition operation will not change the scattering parameters of the filter.

Consider the coupling matrices in Figs. 4 and 5, which, after decomposition, become two separated matrices, as shown in Figs. 6 and 7, respectively. Note from Fig. 6(a) that all the off-diagonal entries in the resistive connection matrix are imaginary, which represent resistive connections among resonators. One should note that, for a series resistor between m^{th} and n^{th} resonators, its coupling matrix is expressed by

$$\begin{bmatrix} -jG_{mn} & jG_{mn} \\ jG_{mn} & -jG_{mn} \end{bmatrix}, \tag{3}$$

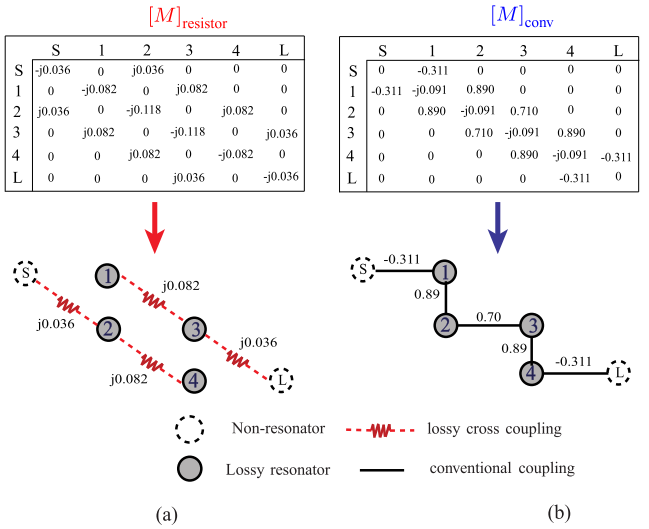

FIGURE 7. Decomposed coupling matrices of a four-pole lossy Chebyshev filter (Fig. 5) (a) resistor connection matrix $[M]_{\text{resistor}}$ with diagram, and (b) residue coupling matrix $[M]_{\text{conv}}$ with corresponding coupling diagram.

where G_{mn} is the conductance. Eq. (3) has non-zero values in the diagonal entries, in contrast to the impedance/admittance inverters having zero diagonal entries. This explains why the resultant resistive connection matrix in Fig. 6(a) have non-zero diagonal entries. On the other hand, the residue matrix in Fig. 6(b) have equal diagonal entries, indicating that all the resonators have the same loss or quality factor, which fulfills the expectation of loss equalization. Also, the off-diagonal entries of the residue matrix are all real and can be implemented by conventional inverters. The decomposed matrices in Fig. 7 have similar properties.

Such a decomposition offers several benefits for the tuning of lossy filters: 1) the decomposition is unique and hence contributes to a quick convergence in the tuning process; 2) it transforms the complex couplings into the form of resistor connection and leaves the residue couplings all real, which eases the tuning; 3) it provides a loss equalized real coupling matrix, which simplifies the implementation; 4) the decomposed two matrices has a one-to-one correspondence with the physical structures, i.e. resistive matrix corresponding to resistors connected among resonators and the residue real coupling matrix corresponding to physically coupled resonators.

C. TUNING PROCEDURE

The tuning procedure for the lossy filters comprises the following steps:

Step 1): Synthesize the coupling matrix using the approach in Sec. II-A, and perform the loss equalization. More details regarding lossy CM synthesis from the specification is provided in [20].

Step 2): Decompose the loss equalized coupling matrix into two parts, i.e. $[M]_{\text{resistor}}$ and $[M]_{\text{conv}}$, following (2). These two matrices are the golden matrices, which represent the ideal targets. Implement the two matrices using the physical structure.

Step 3): Perform the full-wave simulation and check the response. Go to the next step unless the response matches the specification.

Step 4): Sample the scattering parameters from simulation results. Eliminate phase loading error using the phase de-embedding method in [22], and perform bandpass (f) to low pass frequency (Ω) domain transformation.

Step 5): Determine the loss factors, μ_{21}, μ_{11}, and μ_{22}, from magnitude responses of S_{21}, S_{11}, and S_{22}, respectively. For symmetric lossy filters, they are identical, i.e. $\mu_{21} = \mu_{11} = \mu_{22} = K$, as illustrated by the synthesis example in Fig. 5. For asymmetric cases, they are different.

Step 6): Calculate $\Upsilon = S_{21}/S_{11}$ from the lowpass-domain data in *Step 4)* as the objective function and optimize P/F_{11} to match it. Firstly, one calculates $\Upsilon^* = \{\Upsilon_1^*, \Upsilon_2^*, \ldots, \Upsilon_N^*\}$ at N frequencies $\{\Omega_1, \Omega_2, \ldots, \Omega_N\}$, and subsequently applies the following constrained optimization:

$$\text{minimize } \Delta, \quad \text{such that : } \sum_{n=1}^{N} \left\| \frac{P(j\Omega_n)}{F_{11}(j\Omega_n)} - \Upsilon_n^* \right\| \leq \Delta, \quad (4)$$

where Δ is error tolerance, and the optimization parameters are the coefficients of P and F_{11}. The constrained optimization problem (4) is solved using the optimization tool in Matlab.

Step 7): Once P and F_{11} ($= F_{22}$) are obtained, the polynomial E is derived from unitary condition, i.e. $PP^* + F_{11}F_{11}^* = EE^*$.

Step 8): Scale E, P, F_{11}, and F_{22} using the loss factors (μ_p, μ_{11}, μ_{22}) obtained in *Step 5)*. Compute the admittance matrix using these scaled polynomials.

Step 9): Derive the complex coupling matrix from the admittance matrix $[Y]$ obtained in *Step 8)*. Perform the loss equalization.

Step 10): Decompose the loss equalized coupling matrix into two parts, i.e. $[M]_{\text{resistor}}$ and $[M]_{\text{conv}}$, following (2). Compare the two matrices with the targets in *Step 2)* separately. Adjust the resistor values and physical structures following the differences between the extracted matrices and targets. Once updating the physical implementation, go to *Step 3)*.

III. ILLUSTRATIVE EXAMPLE

To further illustrate and demonstrate the proposed tuning method, we physically implement and tune the example in Fig. 5. The specified frequency band is 0.94-1 GHz (a 60 MHz bandwidth centered at 0.97 GHz). The substrate is 1.2-mm-thick Roger RT Duroid-6010 ($\epsilon_r = 10.2$ and $\tan\sigma = 0.0023$).

Following the tuning procedure in Sec. II-C, one firstly obtains the loss equalized coupling matrix and corresponding lowpass responses in Figs. 5(b) and (d), respectively. The complex coupling is further decomposed into two golden matrices in Fig. 7, which are the target matrices one finally reaches. According to the bandpass specification (60 MHz bandwidth centered at 0.97 GHz), the lowpass-domain

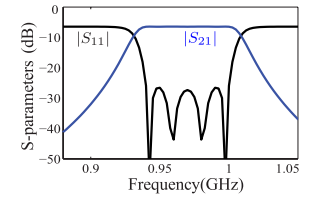

(a)

	S	1	2	3	4	L
S	-j0.0035	-0.0303	j0.0035	0	0	0
1	-0.0303	-j0.0167	0.0864	j0.0080	0	0
2	j0.0035	0.0864	-j0.0202	0.0688	j0.0080	0
3	0	j0.0080	0.0688	-j0.0202	0.0864	j0.0035
4	0	0	j0.0080	0.0864	-j0.0167	-0.0303
L	0	0	0	j0.0035	-0.0303	-j0.0035

(b)

	S	1	2	3	4	L
S	-j0.0035	0	j0.0035	0	0	0
1	0	-j0.0080	0	j0.0080	0	0
2	j0.0035	0	-j0.0115	0	j0.0080	0
3	0	j0.0080	0	-j0.0115	0	j0.0035
4	0	0	j0.0080	0	-j0.0080	0
L	0	0	0	j0.0035	0	-j0.0035

(c)

	S	1	2	3	4	L
S	0	-0.0303	0	0	0	0
1	-0.0303	-j0.0087	0.0864	0	0	0
2	0	0.0864	-j0.0087	0.0688	0	0
3	0	0	0.0688	-j0.0087	0.0864	0
4	0	0	0	0.0864	-j0.0087	-0.0303
L	0	0	0	0	-0.0303	0

(d)

FIGURE 8. Bandpass domain Chebyshev filter as shown in Fig. 7 (a) magnitude responses, (b) complex coupling matrix, (c) resistor connection matrix $[M]_{\text{resistor}}$, (d) residue coupling matrix $[M]_{\text{conv}}$.

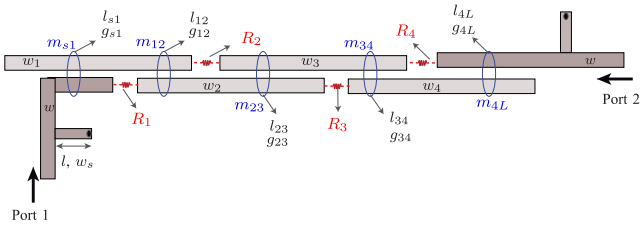

FIGURE 9. Layout showing coupling elements and associated physical parameters used for tuning of lossy four-pole Chebyshev filter as shown in Fig. 8.

matrices in Fig. 5(b) and Fig. 7 are transformed into bandpass-domain matrices in Fig. 8. The corresponding magnitude responses are plotted in Fig. 8(a).

One subsequently implements the resistor connection matrix and conventional coupling matrix of Fig. 8 using the physical structure in Fig. 9. To do this, one firstly implements the conventional coupling matrix in Fig. 8(d) using the coupled microstrip line resonators in Fig. 9, and then connects the resistors between resonators according to the resistor connection matrix in Fig. 8(c). The coupling gap and coupling length are used to control the coupling levels between the adjacent resonators. The resistor values, corresponding to the resistor connection matrix $[M]_{\text{resistor}}$ in Fig. 12(a), is computed by $R_1 = R_4 = 1/(FBW \times [M]^{(S,2)}_{\text{resistor}}) = 885\ \Omega$, where FBW is the fractional bandwidth, and similarly, $R_2 = R_3 = 394\ \Omega$). Since the calculated resistances are not standard values, one may pick the nearest available resistors. Two shorted shunt stubs are used at input/output port to achieve a proper coupling between input/output port and resonators. The computed physical dimensions and resistances of the implemented structure in Fig. 9 are listed in Tab. 4.

Once having the physical structure in Fig. 9, one performs the full-wave EM simulation using Advanced Design System (ADS) and computes the magnitude responses in Fig. 10(a), which do not agree with the ideal ones in Fig. 8(a). Therefore, one goes to Step 3) of the tuning procedure in Sec. II-C.

One firstly samples the frequency responses of Fig. 10(a) within the passband using 51 points and removes the phase

TABLE 4. All initial dimensions (mm) used in tuning cycle: 1.

Coupling Gaps	$g_{s1} = 1.5$, $g_{12} = 2.0$, $g_{23} = 2.0$, $g_{34} = 2.0$, $g_{4L} = 1.5$
Coupling Lengths	$l_{s1} = 10$, $l_{12} = 15$, $l_{23} = 20$, $l_{34} = 20$, $l_{4L} = 10$, $l = 5.0$
Line Widths	$w_s = 0.5$, w_1 =w_2=w_3=w_4=1.3, $w = 1.3$
Resistors	$R_1 = R_4 = 910\ \Omega$, $R_2 = R_3 = 390\ \Omega$

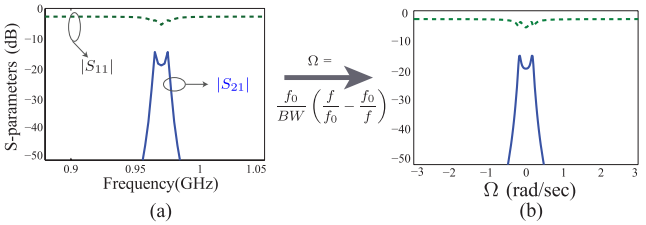

(a) (b)

FIGURE 10. BP to low pass frequency transformation (a) bandpass domain (f) magnitude responses, and (b) lowpass domain (Ω) magnitude responses.

TABLE 5. Extracted characteristic polynomials from Fig. 10 (b).

$P'(s)$	$j0.00012$
$F'_{11}(s) = F'_{22}(s)$	$0.711s^4 + 0.317s^3 + 0.640s^2 + 0.011s + 0.0007$
$E(s)$	$s^4 + 0.445s^3 + 0.905s^2 + 0.0155s + 0.0011$

	S	1	2	3	4	L
S	-j0.1537	-0.1723	0	0	0	0
1	-0.1723	-j0.1801	0.1111	0	0	0
2	0	0.1111	0	0.1501	0	0
3	0	0	0.1501	0	0.1102	0
4	0	0	0	0.1102	-j0.1801	-0.3717
L	0	0	0	0	-0.3717	-j0.1537

(a)

	S	1	2	3	4	L
S	-j0.0192	-0.0638	j0.0192	0	0	0
1	-0.0638	-j0.0797	0.0737	j0.0270	0	0
2	j0.0192	0.0737	-j0.0989	0.1650	j0.0270	0
3	0	j0.0270	0.1650	-j0.0989	0.0732	j0.0192
4	0	0	j0.0270	0.0732	-j0.0797	-0.1377
L	0	0	0	j0.0192	-0.1377	-j0.0192

(b)

FIGURE 11. Computed coupling matrices from Table 5 (a) CM before loss equalization, and (b) CM after loss equalization.

	S	1	2	3	4	L
S	-j0.0192	0	j0.0192	0	0	0
1	0	-j0.0270	0	j0.0270	0	0
2	j0.0192	0	-j0.0462	0	j0.0270	0
3	0	j0.0270	0	-j0.0462	0	j0.0192
4	0	0	j0.0270	0	-j0.0270	0
L	0	0	0	j0.0192	0	-j0.0192

(a)

	S	1	2	3	4	L
S	0	-0.0638	0	0	0	0
1	-0.0638	-j0.0527	0.0737	0	0	0
2	0	0.0737	-j0.0527	0.1650	0	0
3	0	0	0.1650	-j0.0527	0.0732	0
4	0	0	0	0.0732	-j0.0527	-0.1377
L	0	0	0	0	-0.1377	0

(b)

FIGURE 12. Decomposed coupling matrices of Fig. 11(b) (a) resistor connection matrix $[M]_{\text{resistor}}$, and (b) residue coupling matrix $[M]_{\text{conv}}$.

loading error using the phase de-embedding method in [22]. One subsequently applies the bandpass-to-lowpass transformation to the response in Fig. 10(a), and obtains the lowpass-domain responses in Fig. 10(b). Then, one computes the loss factors, $\mu_{21} = 0.563$, and $\mu_{11} = \mu_{22} = 0.710$. Next, one applies the optimization in (4) and unitary condition to computes P, F_{11} and E, as shown in Tab. 5.

The obtained polynomials are further transformed into coupling matrices in Fig. 11. Finally, the loss equalized coupling matrix in Fig. 11(b) is decomposed into a resistor

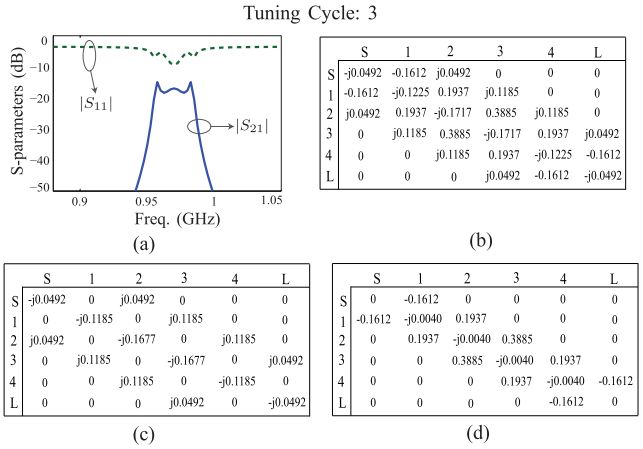

	S	1	2	3	4	L
S	-j0.0492	-0.1612	j0.0492	0	0	0
1	-0.1612	-j0.1225	0.1937	j0.1185	0	0
2	j0.0492	0.1937	-j0.1717	0.3885	j0.1185	0
3	0	j0.1185	0.3885	-j0.1717	0.1937	j0.0492
4	0	0	j0.1185	0.1937	-j0.1225	-0.1612
L	0	0	0	j0.0492	-0.1612	-j0.0492

	S	1	2	3	4	L
S	-j0.0492	0	j0.0492	0	0	0
1	0	-j0.1185	0	j0.1185	0	0
2	j0.0492	0	-j0.1677	0	j0.1185	0
3	0	j0.1185	0	-j0.1677	0	j0.0492
4	0	0	j0.1185	0	-j0.1185	0
L	0	0	0	j0.0492	0	-j0.0492

	S	1	2	3	4	L
S	0	-0.1612	0	0	0	0
1	-0.1612	-j0.0040	0.1937	0	0	0
2	0	0.1937	-j0.0040	0.3885	0	0
3	0	0	0.3885	-j0.0040	0.1937	0
4	0	0	0	0.1937	-j0.0040	-0.1612
L	0	0	0	0	-0.1612	0

FIGURE 13. Responses and corresponding matrices in the 3rd tuning cycle (a) magnitude responses, (b) extracted complex coupling matrix, (c) resistor connection matrix $[M]_{resistor}$, and (d) residue coupling matrix $[M]_{conv}$.

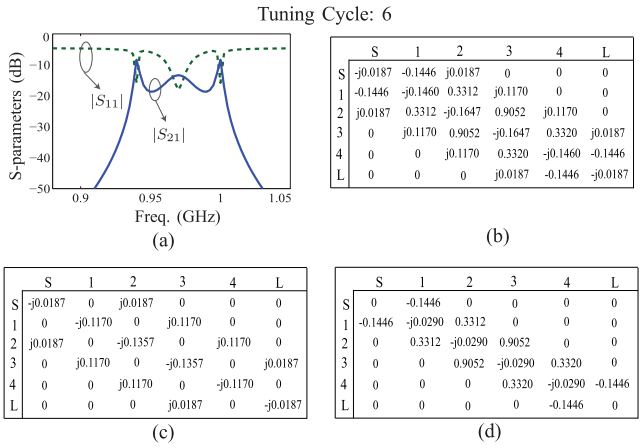

	S	1	2	3	4	L
S	-j0.0187	-0.1446	j0.0187	0	0	0
1	-0.1446	-j0.1460	0.3312	j0.1170	0	0
2	j0.0187	0.3312	-j0.1647	0.9052	j0.1170	0
3	0	j0.1170	0.9052	-j0.1647	0.3320	j0.0187
4	0	0	j0.1170	0.3320	-j0.1460	-0.1446
L	0	0	0	j0.0187	-0.1446	-j0.0187

	S	1	2	3	4	L
S	-j0.0187	0	j0.0187	0	0	0
1	0	-j0.1170	0	j0.1170	0	0
2	j0.0187	0	-j0.1357	0	j0.1170	0
3	0	j0.1170	0	-j0.1357	0	j0.0187
4	0	0	j0.1170	0	-j0.1170	0
L	0	0	0	j0.0187	0	-j0.0187

	S	1	2	3	4	L
S	0	-0.1446	0	0	0	0
1	-0.1446	-j0.0290	0.3312	0	0	0
2	0	0.3312	-j0.0290	0.9052	0	0
3	0	0	0.9052	-j0.0290	0.3320	0
4	0	0	0	0.3320	-j0.0290	-0.1446
L	0	0	0	0	-0.1446	0

FIGURE 14. Responses and corresponding matrices in the 6th tuning cycle: (a) magnitude responses, (b) extracted complex coupling matrix, (c) resistor connection matrix $[M]_{resistor}$, and (d) residue coupling matrix $[M]_{conv}$.

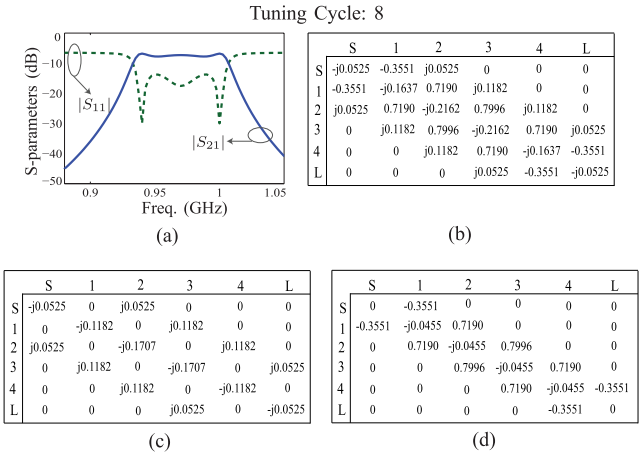

	S	1	2	3	4	L
S	-j0.0525	-0.3551	j0.0525	0	0	0
1	-0.3551	-j0.1637	0.7190	j0.1182	0	0
2	j0.0525	0.7190	-j0.2162	0.7996	j0.1182	0
3	0	j0.1182	0.7996	-j0.2162	0.7190	j0.0525
4	0	0	j0.1182	0.7190	-j0.1637	-0.3551
L	0	0	0	j0.0525	-0.3551	-j0.0525

	S	1	2	3	4	L
S	-j0.0525	0	j0.0525	0	0	0
1	0	-j0.1182	0	j0.1182	0	0
2	j0.0525	0	-j0.1707	0	j0.1182	0
3	0	j0.1182	0	-j0.1707	0	j0.0525
4	0	0	j0.1182	0	-j0.1182	0
L	0	0	0	j0.0525	0	-j0.0525

	S	1	2	3	4	L
S	0	-0.3551	0	0	0	0
1	-0.3551	-j0.0455	0.7190	0	0	0
2	0	0.7190	-j0.0455	0.7996	0	0
3	0	0	0.7996	-j0.0455	0.7190	0
4	0	0	0	0.7190	-j0.0455	-0.3551
L	0	0	0	0	-0.3551	0

FIGURE 15. Responses and corresponding matrices in the 8th tuning cycle: (a) magnitude responses, (b) extracted complex coupling matrix, (c) resistor connection matrix $[M]_{resistor}$, and (d) residue coupling matrix $[M]_{conv}$.

connection matrix and a conventional coupling matrix in Fig. 12, which, after being compared with the golden matrices in Fig. 7, indicate how to tune the physical parameters

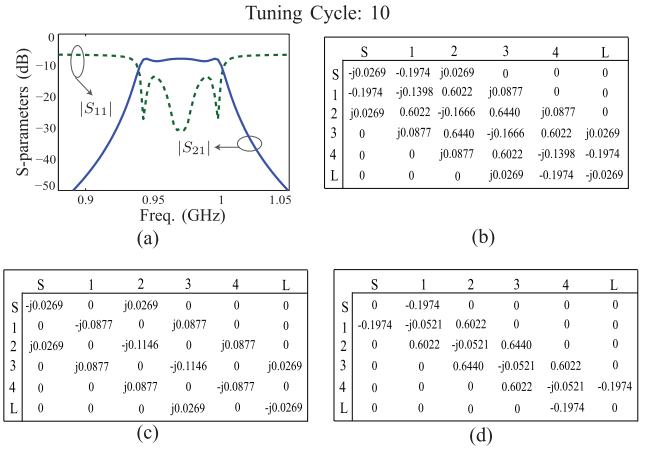

	S	1	2	3	4	L
S	-j0.0269	-0.1974	j0.0269	0	0	0
1	-0.1974	-j0.1398	0.6022	j0.0877	0	0
2	j0.0269	0.6022	-j0.1666	0.6440	j0.0877	0
3	0	j0.0877	0.6440	-j0.1666	0.6022	j0.0269
4	0	0	j0.0877	0.6022	-j0.1398	-0.1974
L	0	0	0	j0.0269	-0.1974	-j0.0269

	S	1	2	3	4	L
S	-j0.0269	0	j0.0269	0	0	0
1	0	-j0.0877	0	j0.0877	0	0
2	j0.0269	0	-j0.1146	0	j0.0877	0
3	0	j0.0877	0	-j0.1146	0	j0.0269
4	0	0	j0.0877	0	-j0.0877	0
L	0	0	0	j0.0269	0	-j0.0269

	S	1	2	3	4	L
S	0	-0.1974	0	0	0	0
1	-0.1974	-j0.0521	0.6022	0	0	0
2	0	0.6022	-j0.0521	0.6440	0	0
3	0	0	0.6440	-j0.0521	0.6022	0
4	0	0	0	0.6022	-j0.0521	-0.1974
L	0	0	0	0	-0.1974	0

FIGURE 16. Responses and corresponding matrices in the 10th tuning cycle (a) magnitude responses, (b) extracted complex coupling matrix, (c) resistor connection matrix $[M]_{resistor}$, and (d) residue coupling matrix $[M]_{conv}$.

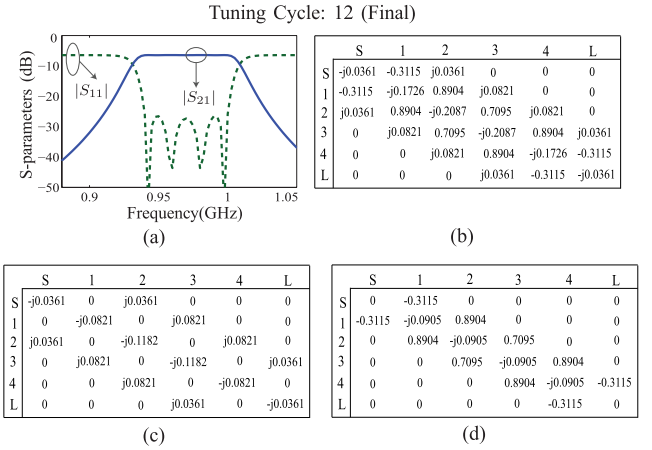

	S	1	2	3	4	L
S	-j0.0361	-0.3115	j0.0361	0	0	0
1	-0.3115	-j0.1726	0.8904	j0.0821	0	0
2	j0.0361	0.8904	-j0.2087	0.7095	j0.0821	0
3	0	j0.0821	0.7095	-j0.2087	0.8904	j0.0361
4	0	0	j0.0821	0.8904	-j0.1726	-0.3115
L	0	0	0	j0.0361	-0.3115	-j0.0361

	S	1	2	3	4	L
S	-j0.0361	0	j0.0361	0	0	0
1	0	-j0.0821	0	j0.0821	0	0
2	j0.0361	0	-j0.1182	0	j0.0821	0
3	0	j0.0821	0	-j0.1182	0	j0.0361
4	0	0	j0.0821	0	-j0.0821	0
L	0	0	0	j0.0361	0	-j0.0361

	S	1	2	3	4	L
S	0	-0.3115	0	0	0	0
1	-0.3115	-j0.0905	0.8904	0	0	0
2	0	0.8904	-j0.0905	0.7095	0	0
3	0	0	0.7095	-j0.0905	0.8904	0
4	0	0	0	0.8904	-j0.0905	-0.3115
L	0	0	0	0	-0.3115	0

FIGURE 17. Responses and corresponding matrices in the 12th tuning cycle (a) magnitude responses, (b) extracted complex coupling matrix, (c) resistor connection matrix $[M]_{resistor}$, and (d) residue coupling matrix $[M]_{conv}$.

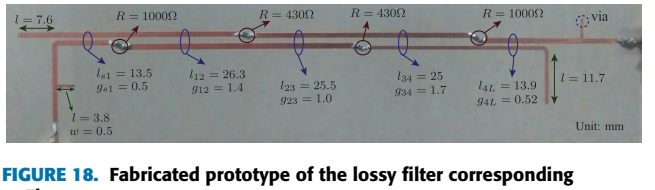

FIGURE 18. Fabricated prototype of the lossy filter corresponding to Fig. 17.

in Fig. 9. For instance, the entry (2,3) in Fig. 12(b) (0.165) is smaller than the one in the golden matrix of Fig. 7(b) (0.710), indicating that one needs to decrease g_{23} or increase l_{23} of Fig. 9 to enhance the coupling level between the 2nd and 3rd resonators. By updating all the physical parameters using this strategy, one goes to the next cycle of tuning until the responses match the specification. Figs. 13-17 shows the responses and extracted coupling matrices in different tuning cycles. One runs twelve cycles to obtain a good response that matches the specification.

To experimentally validate the physical implementation in Fig. 9, we fabricate a prototype in Fig. 18. The dimensions

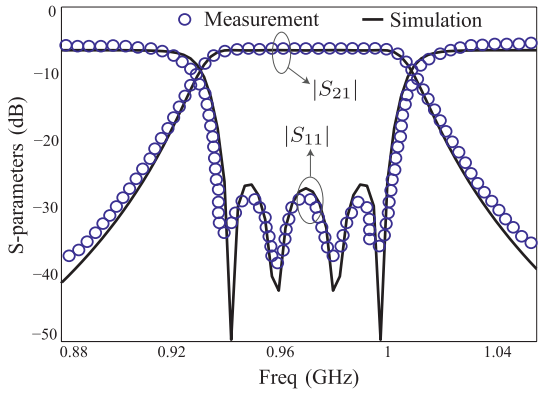

FIGURE 19. Measured scattering parameter responses of the fabricated prototype as shown in Fig. 18 (the corresponding coupling matrix and scattering parameters are given in Fig. 17).

are obtained after 12 tuning cycles. The final transmission and reflection responses are measured in a vector network analyzer. Fig. 19 shows the measured responses in comparison with the simulated ones in Fig. 17(a). The good agreement between the measured and simulated responses finally demonstrates the validity of the tuned lossy filter.

IV. CONCLUSION

In this paper, the tuning technique for highly lossy filters has been proposed and demonstrated for the first time. A decomposition technique has been introduced in context of lossy filter tuning method. Parallel tuning of lossy and lossless couplings has been achieved by applying the decomposition method. A numerical example with experimental validation has been presented to illustrate and validate the proposed tuning technique.

REFERENCES

[1] A. E. Atia and A. E. Williams, "Narrow-bandpass waveguide filters," *IEEE Trans. Microw. Theory Techn.*, vol. 20, no. 4, pp. 258–265, Apr. 1972.

[2] R. J. Cameron, "General coupling matrix synthesis methods for Chebyshev filtering functions," *IEEE Trans. Microw. Theory Techn.*, vol. 47, no. 4, pp. 433–442, Apr. 1999.

[3] R. J. Cameron, "Advanced coupling matrix synthesis techniques for microwave filters," *IEEE Trans. Microw. Theory Techn.*, vol. 51, no. 1, pp. 1–10, Jul. 2003.

[4] R. Cameron, C. Kudsia, and R. Mansour, *Microwave Filters for Communication Systems: Fundamentals, Design, and Applications*, vol. 1. Hoboken, NJ, USA: Wiley, 2007.

[5] L. Accatino, "Computer-aided tuning of microwave filters," in *IEEE MTT-S Int. Microw. Symp. Dig.*, Jun. 1986, pp. 249–252.

[6] J. B. Ness, "A unified approach to the design, measurement, and tuning of coupled-resonator filters," *IEEE Trans. Microw. Theory Techn.*, vol. 46, no. 4, pp. 343–351, Apr. 1998.

[7] H.-T. Hsu, H.-W. Yao, K. A. Zaki, and A. E. Atia, "Computer-aided diagnosis and tuning of cascaded coupled resonators filters," *IEEE Trans. Microw. Theory Techn.*, vol. 50, no. 4, pp. 1137–1145, Apr. 2002.

[8] G. Pepe, F. J. Gortz, and H. Chaloupka, "Sequential tuning of microwave filters using adaptive models and parameter extraction," *IEEE Trans. Microw. Theory Techn.*, vol. 53, no. 1, pp. 22–31, Jan. 2005.

[9] V. Miraftab and R. R. Mansour, "Computer-aided tuning of microwave filters using fuzzy logic," *IEEE Trans. Microw. Theory Techn.*, vol. 50, no. 12, pp. 2781–2788, Dec. 2002.

[10] V. Miraftab and R. R. Mansour, "A robust fuzzy-logic technique for computer-aided diagnosis of microwave filters," *IEEE Trans. Microw. Theory Techn.*, vol. 52, no. 1, pp. 450–456, Jan. 2004.

[11] V. Miraftab and R. R. Mansour, "Computer-aided tuning of microwave filters using fuzzy logic," in *IEEE MTT-S Int. Microw. Symp. Dig.*, vol. 2, Jun. 2002, pp. 1117–1120.

[12] V. Miraftab and R. R. Mansour, "Tuning of microwave filters by extracting human experience using fuzzy logic," in *IEEE MTT-S Int. Microw. Symp. Dig.*, Jun. 2005, pp. 1605–1608.

[13] V. Miraftab and R. R. Mansour, "Automated microwave filter tuning by extracting human experience in terms of linguistic rules using fuzzy controllers," in *IEEE MTT-S Int. Microw. Symp. Dig.*, Jun. 2006, pp. 1439–1442.

[14] V. Miraftab and R. R. Mansour, "Fully automated RF/microwave filter tuning by extracting human experience using fuzzy controllers," *IEEE Trans. Circuits Syst. I, Reg. Papers*, vol. 55, no. 5, pp. 1357–1367, Jun. 2008.

[15] L.-H. Hsieh and K. Chang, "Dual-mode quasi-elliptic-function bandpass filters using ring resonators with enhanced-coupling tuning stubs," *IEEE Trans. Microw. Theory Techn.*, vol. 50, no. 5, pp. 1340–1345, May 2002.

[16] J. Zhou, G. Zhang, and M. J. Lancaster, "Passive microwave filter tuning using bond wires," *IET Microw., Antennas Propag.*, vol. 1, no. 3, pp. 567–571, Jun. 2007.

[17] R. Das, Q. Zhang, and H. Liu, "Lossy coupling matrix synthesis approach for the realization of negative group delay response," *IEEE Access*, vol. 6, pp. 1916–1926, 2018.

[18] M. Meng and K. L. Wu, "An analytical approach to computer-aided diagnosis and tuning of lossy microwave coupled resonator filters," *IEEE Trans. Microw. Theory Techn.*, vol. 57, no. 12, pp. 3188–3195, Dec. 2009.

[19] R. Das, Q. Zhang, A. Kandwal, and H. Liu, "Coupling matrix extraction technique for auto tuning of highly lossy filters," in *IEEE MTT-S Int. Microw. Symp. Dig.*, Jun. 2018, pp. 697–700.

[20] V. Miraftab and M. Yu, "Advanced coupling matrix and admittance function synthesis techniques for dissipative microwave filters," *IEEE Trans. Microw. Theory Techn.*, vol. 57, no. 10, pp. 2429–2438, Oct. 2009.

[21] A. C. Guyette, I. C. Hunter, and R. D. Pollard, "The design of microwave bandpass filters using resonators with nonuniform Q," *IEEE Trans. Microw. Theory Techn.*, vol. 54, no. 11, pp. 3914–3922, Nov. 2006.

[22] H. Hu and K.-L. Wu, "A generalized coupling matrix extraction technique for bandpass filters with uneven-Qs," *IEEE Trans. Microw. Theory Techn.*, vol. 62, no. 2, pp. 244–251, Feb. 2014.

RANJAN DAS received the B.E. degree in electronics and instrumentation engineering from Jadavpur University and the master's degree from the Electrical Engineering Department, IIT Bombay, Mumbai, in 2013, with a focus on electronics systems design, where he is currently pursuing the Ph.D. degree. In 2016, he joined the Electronics and Electrical Engineering Department, South University of Science and Technology of China, Shenzhen, China, as a Visiting Student. His research area includes reconfigurable multiband filter design, and synthesis of negative group delay circuits. He is also interested in real time analog signal processing for microwave frequencies.

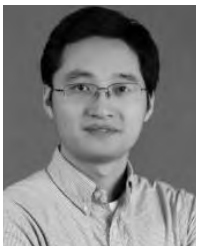

QINGFENG ZHANG (S'07–M'11–SM'15) received the B.E. degree in electrical engineering from the University of Science and Technology of China, Hefei, China, in 2007, and the Ph.D. degree in electrical engineering from Nanyang Technological University, Singapore, in 2011.

From 2011 to 2013, he was with the Poly-Grames Research Center, École Polytechnique de Montréal, Montreal, Canada, as a Post-Doctoral Fellow. Since 2013, he has been with the Southern University of Science and Technology, Shenzhen, China, as an Assistant Professor.

His research interests are focused on emerging novel electromagnetics technologies and multidisplininary topics. He has authored/co-authored over 150 research papers. He has served as the Vice-Chair of the IEEE AP-S Shenzhen Chapter. He has been an Associate Editor of the IEEE Access since 2017, and a Lead Guest Editor of the *International Journal of Antennas and Propagation* from 2014 to 2015. He was the Publication Chair of the IEEE ICCS in 2016, a Local Organization Committee Co-Chair of the IEEE EDAPS 2017, and TPC members of many international conferences.

Dr. Zhang received the URSI Young Scientist Award in URSI-ATRASC 2018 and the ACES Young Scientist Award in ACES-China 2018.

ABHISHEK KANDWAL received the master's degree (Hons.) in physics with a specialization in nuclear and particle physics from Himachal Pradesh University, Shimla, India, in 2009, and the Ph.D. degree in microstrip antennas for communication systems from the Jaypee University of Information Technology, India, in 2014. During his Ph.D., he has also worked in a three-year project on antennas from the Defence Research and Development Organization, India. From 2014 to 2016, he was a Post-Doctoral Fellow with the National Electronics and Computer Technology Centre, NSTDA, MOST, Thailand. He has also worked in a project on radars from the Defence Technology Institute, Thailand, during his post-doctoral position. In 2016, he joined the Prof. Zhang's Research Group as a Post-Doctoral Fellow with the Electronics and Electrical Engineering Department, Southern University of Science and Technology, Shenzhen, China. His research is focused on advanced antenna's for microwave, mm-wave and THz for applications including communications systems for mobile, Wi-Fi, 5G, satellites, and radars.

HAIWEN LIU (M'04–SM'13) received the B.S. degree in electronic system and the M.S. degree in radio physics from Wuhan University, Wuhan, China, in 1997 and 2000, respectively, and the Ph.D. degree in microwave engineering from Shanghai Jiao Tong University, Shanghai, China, in 2004.

From 2004 to 2006, he was a Research Assistant Professor with Waseda University, Kitakyushu, Japan. From 2006 to2007, he was a Research Fellow with Kiel University, Kiel, Germany, where he was granted the Alexandervon Humboldt Research Fellowship . From 2007 to 2008, he was a Professor with the Institute of Optics and Electronics, Chengdu, China, where he was supported by the100 Talents Program of the Chinese Academy of Sciences, Beijing, China. From 2009 to 2017, he was a Chair Professor with East China Jiaotong University, Nanchang, China. Since 2017, he has been a Professor with Xi'an Jiaotong University, Xi'an, China. He has authored over 100 papers in international and domestic journals and conferences. His current research interests include the electromagnetic modeling of high-temperature superconducting circuits, radiofrequency and microwave passive circuits and systems, synthesis theory and practices of microwave filters and devices, antennas for wireless terminals, and radar systems.

YIFAN CHEN received the B.Eng. (Hons.) and Ph.D. degrees in electrical and electronic engineering from Nanyang Technological University, Singapore, in 2002 and 2006, respectively. From 2005 to 2007, he was a Project Officer and then a Research Fellow with the Singapore-University of Washington Alliance in Bioengineering, supported by the Singapore Agency for Science, Technology and Research, Nanyang Technological University, and the University of Washington at Seattle, USA. From 2007 to 2012, he was a Lecturer and then a Senior Lecturer with the University of Greenwich and Newcastle University, U.K. From 2012 to 2016, he was a Professor and the Head of the Department of Electrical and Electronic Engineering, Southern University of Science and Technology, Shenzhen, China, appointed through the Recruitment Program of Global Experts (known as the Thousand Talents Plan). In 2013, he was a Visiting Professor with the Singapore University of Technology and Design, Singapore. He is currently with The University of Waikato, Hamilton, New Zealand, as a Professor of engineering, where he is also the Associate Dean External Engagement for the Faculty of Science and Engineering and the Faculty of Computing and Mathematical Sciences, The University of Waikato.